Both Ca^{2+}-permeable and -impermeable AMPA receptors contribute to primary synaptic drive onto rat dorsal horn neurons

Chi-Kun Tong and Amy B. MacDermott

Department of Physiology and Cellular Biophysics and the Center for Neurobiology and Behavior, Columbia University, New York, NY 10032, USA

Blockade of Ca^{2+}-permeable AMPA receptors in the rat spinal cord diminishes the development of hyperalgesia and allodynia associated with peripheral injury. Cobalt uptake studies reveal that Ca^{2+}-permeable AMPA receptors are expressed by some substance P receptor-expressing (NK1R+) neurons in lamina I, as well as other neurons throughout the superficial dorsal horn. Selective elimination of NK1R+ neurons in lamina I and lamina III/IV of the dorsal horn also suppresses development of hyperalgesia and allodynia. These observations raise the possibility that Ca^{2+}-permeable AMPA receptors contribute to excitatory synaptic drive onto the NK1R+ neurons associated with allodynia and hyperalgesia. The first synapse in the pain pathway is the glutamatergic excitatory drive from the primary afferent fibres onto dorsal horn neurons. Therefore, we tested whether Ca^{2+}-permeable AMPA receptors are located on lamina I and lamina III/IV NK1R+ neurons postsynaptic to primary afferent fibres, using inward rectification and polyamine toxins for receptor identification. We examined three different populations of dorsal horn neurons; lamina I NK1R+ neurons, including projection neurons, and non-NK1R+ (NK1R–) neurons including interneurons, and lamina III/IV NK1R+ neurons, believed to contribute to the low-threshold mechanosensory pathway. The majority of synapses in all three groups had rectification indices less than 1.0 and greater than 0.4, indicating that the AMPA receptors at these synapses are a mixture of Ca^{2+}-permeable and -impermeable forms. Lamina III/IV NK1R+ neurons and lamina I NK1R– neurons have a significantly higher proportion of postsynaptic Ca^{2+}-permeable AMPA receptors than lamina I NK1R+ neurons. Thus synaptically positioned Ca^{2+}-permeable AMPA receptors directly contribute to low-threshold sensory afferent drive into the dorsal horn, and can mediate afferent input onto interneurons such as GABAergic neurons. These receptors also contribute to high-threshold primary afferent drive onto NK1R+ neurons in the superficial dorsal horn, but do so less consistently.

(Received 24 March 2006; accepted after revision 5 June 2006; first published online 8 June 2006)
Corresponding author C.-K. Tong: Department of Physiology and Cellular Biophysics, Columbia University, 630 W. 168th St, Room 1109, New York, NY 10032, USA. Email: ct433@columbia.edu

Hyperalgesia and allodynia resulting from inflammation and nerve injury involve complex interactions among different cellular elements in the dorsal horn. The underlying mechanisms have been under intensive study. First-degree burn causes secondary mechanical allodynia (Jones & Sorkin, 2004), while gastrocnemius incision causes secondary mechanical hyperalgesia (Pogatzki *et al.* 2003) in rat models. Both of these pain hypersensitivities can be abolished by the antagonist for Ca^{2+}-permeable AMPA receptors, Joro spider toxin, JSTX (Pogatzki *et al.* 2003; Jones & Sorkin, 2004). Elevated expression of Ca^{2+}-permeable AMPA receptors in GluR2-deficient mice facilitates nociceptive plasticity and enhances hyperalgesia (Hartmann *et al.* 2004), suggesting that these receptors are important for development of enhanced pain responses. Interestingly, selective elimination of substance P receptor-expressing (NK1R+) neurons in lamina I and lamina III/IV by intrathecal injection of substance P-conjugated cytotoxin, saporin, also diminishes the development of thermal hyperalgesia and mechanical allodynia (Nichols *et al.* 1999). Some NK1R+ neurons in lamina I and some lamina III/IV neurons express Ca^{2+}-permeable AMPA receptors as demonstrated by cobalt loading experiments (Engelman

 DOI: 10.1113/jphysiol.2006.110072

et al. 1999). Given the critical role of the NK1R+ neurons in expression of allodynia and hyperalgesia, we directly tested the hypothesis that Ca^{2+}-permeable AMPA receptors mediate primary afferent excitatory drive onto them. We tested this at both high-threshold inputs onto lamina I NK1R+ neurons, and at the predominantly low-threshold inputs onto lamina III NK1R+ neurons. For comparison, and because many of the non-NK1R+ (NK1R–) neurons in lamina I also show evidence for Ca^{2+}-permeable AMPA receptor expression (Engelman *et al.* 1999), we investigated the AMPA receptors mediating the primary afferent inputs onto this neuronal group. Our results demonstrate that lamina III/IV NK1R+ neurons and lamina I NK1R– neurons have a significantly higher percentage of postsynaptic AMPA receptors that are permeable to Ca^{2+} at primary afferent synapses than lamina I NK1R+ neurons.

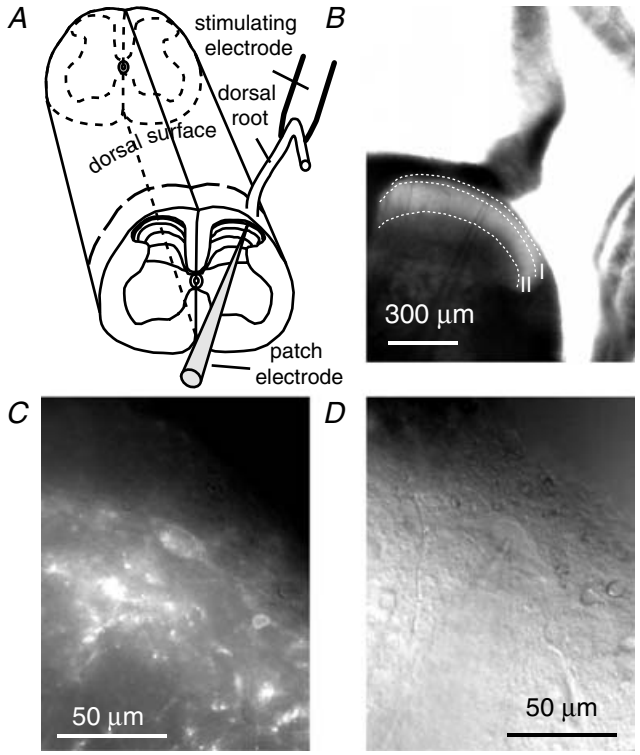

Figure 1. Transverse slice selectively labelled by TMR-substance P shows an NK1 receptor-expressing neuron (NK1R+ neuron) in the superficial dorsal horn
A, diagram illustrates transverse slicing of the rat spinal cord preparation. The dashed line on the dorsal surface of the spinal cord shows the orientation of slicing. *B*, transverse slice and a patch pipette under low magnification (×4 objective). I and II indicate dorsal horn lamina I and lamina II, respectively. *C*, fluorescence image of the NK1R+ dorsal horn neuron (×40 objective). *D*, IR-DIC image of the same area as in *C*, showing the NK1R+ neuron patched with the patch pipette.

Methods

Transverse slice preparation

Lumbar spinal cords with attached dorsal roots were obtained from rats of postnatal day 13 (P13) to P23. The animals were first fully anaesthetized with 100% isoflurane (350–400 μl) inhalation in a small chamber ($\sim$400 cm^3) and then decapitated. All experiments were conducted with the approval of the Columbia University Institutional Animal Care and Use Committee and in accord with the *Guide for the Care and Use of Laboratory Animals*. The spinal cords were excised and placed in ice-cold oxygenated high-Mg^{2+} Krebs solution (95% O_2–5% CO_2 saturated Krebs solution, mM: NaCl 125, KCl 2.5, $NaHCO_3$ 26, NaH_2PO_4 1.25, glucose 25, $MgCl_2$ 6, $CaCl_2$ 1.5, pH 7.4) plus 1 mM kynurenic acid. After removal of the dura mater and arachnoid membrane, all ventral roots were cut close to the cord, and the spinal cord was embedded in low-melting agarose (Invitrogen Life Technologies) for slicing. Transverse slices (350–400 μm) with attached dorsal roots were obtained using a Leica VT1000S vibrating blade microtome. Figure 1*A* and *B* shows the direction of slicing and a transverse slice under low magnification (×4), respectively. Slices were then incubated in oxygenated high-Mg^{2+} Krebs solution at 35°C for at least 1 h, then used at room temperature. Normal 95% O_2–5% CO_2-saturated Krebs solution was used for recording. It comprised (mM): NaCl 125, KCl 2.5, NaH_2PO_4 1.25, $NaHCO_3$ 26, glucose 25, $MgCl_2$ 1, $CaCl_2$ 2, pH 7.4.

Recording from pre-identified NK1R+ neurons

To label NK1R+ dorsal horn neurons with fluorescent dye, spinal cord slices were incubated in high-Mg^{2+} Krebs solution containing 20 nM tetramethylrhodamine-conjugated substance P (TMR-substance P) for 20–30 min at room temperature after 1 h of recovery at 35°C. After unbound substance P was washed away for at least 20 min in an incubation chamber, slices were transferred to a submersion-style chamber for recording (Labrakakis & MacDermott, 2003). NK1R+ dorsal horn neurons were visually identified with Chroma HQ-CY3 filter set (exciter: HQ545/30, emitter: HQ610/75, beamsplitter: Q570LP). As shown in Fig. 1*C* and *D*, NK1R+ neurons of spinal cord slices were readily identified for patch-clamp recording in whole-cell configuration. Recordings were made at room temperature. Intracellular solution had the following composition (mM): Cs-methylsulphonate 130, Na-methylsulphonate 10, EGTA 10, $CaCl_2$ 1, Hepes 10, QX-314·Cl 5, spermine tetrahydrochloride 0.1, Mg^{2+}-ATP 2, pH adjusted to 7.2 with CsOH, osmolarity adjusted to 290 mosmol l^{-1} with sucrose. The typical resistances for the patch electrodes were 3–4 MΩ.

Cells were held at −70 mV under voltage-clamp control unless otherwise specified. Synaptic currents were recorded at different membrane potentials from −90 mV to +50 mV using 20 mV steps. Junction potentials were corrected in the bath before gigaohm seal formation for each cell. Dorsal roots were stimulated using a glass suction electrode as shown in Fig. 1*A*. In most cases, stimulation intensities ranged from 70 to 400 μA for lamina I neurons and 30–120 μA for lamina III/IV neurons (constant current output, and consisted of 0.1 ms duration at frequencies between 0.03 and 0.05 Hz, see Results). Stimulus intensity was gradually increased until the maximal response was identified. The intensity was then adjusted slightly higher to ensure consistent axon activation under control conditions. Monosynaptic responses were selected based on the absence of synaptic failures and low variability of latency at a stimulation frequency of 10 Hz. Specifically, variation of the latency for evoked responses was required to be less than 15% of the mean latency for the synaptic currents using 5–10 stimuli at 10 Hz. At this frequency, polysynaptic responses tended to fail, and markedly changed their latency while monosynaptic responses kept a constant latency. The latency was defined as the time interval between the stimulus artifact and the response onset. Latency values ranged from 3 to 14 ms for lamina I NK1R+ neurons, 2–10 ms for lamina I NK1R– neurons, and 1.8–3.5 ms for lamina III NK1R+ neurons. Neurons with high or low reversal potentials ($>$ 8 mV or $<$ –8 mV) for AMPA excitatory postsynaptic currents (EPSCs) were not included in the analysis.

Excitatory postsynaptic current (EPSC) recording and analysis

Data were recorded and acquired using a Digidata 1322A, an Axopatch 200 amplifier and pCLAMP 9.0 software (Axon instruments, Union City, CA, USA). Sampling rate was 10–20 kHz, and data were filtered at 5 kHz. To study evoked EPSCs at different voltages, the membrane potential was stepped to a new value 350 ms before giving a stimulus to the dorsal root. To isolate the synaptic current, membrane currents recorded in the absence of a dorsal root stimulation at each membrane potential were subtracted from the synaptic record. Clampfit 9.0 software (Axon instruments) was used to analyse evoked synaptic currents.

Peak amplitude measurement of synaptic currents was performed on averages of three evoked EPSCs. When evoked AMPA receptor-mediated EPSCs (AMPA EPSCs) had multiple peaks, only the first peak was measured and analysed. To calculate the rectification index (RI) of the AMPA EPSCs, the peak conductance of AMPA EPSCs at +50 mV (g_{+50}) was divided by the peak conductance (g_{-50}) of EPSCs at −50 mV based on the following equation:

$$\mathrm{RI} = g_{+50}/g_{-50} = (I_{+50}/(50 - E_{\mathrm{rev}}))/(I_{-50}/(50 + E_{\mathrm{rev}}))$$

Because E_{rev} is ∼0 mV:

$$\mathrm{RI} = g_{+50}/g_{-50} \cong I_{+50}/I_{-50}$$

An RI $<$ 1 indicates an inward rectification of this synapse, while an RI $>$ 1 indicates an outward rectification.

The rise time of an AMPA EPSC was measured from 10% to 90% of the peak amplitude.

Data were expressed as means ± standard error of the mean, with n referring to the number of cells. A paired t test was used to test the significance of average attenuating effect of drugs. Fisher's least significant difference (LSD) test was used for multiple comparisons.

Materials

SYM 2081, D-APV, SR 95531 hydrobromide, HPP-spermine, and spermine tetrahydrochloride were purchased from Tocris Cookson (Bristol, UK). QX-314·Cl was purchased from Alomone Labs (Jerusalem, Israel). Low-melting-point agarose and TMR-substance P were purchased from Invitrogen Corp. Strychnine, synthetic Joro spider toxin (JSTX-3), philanthotoxin-433 and GYKI 52466 were obtained from Sigma-Aldrich. GYKI 53655 was a gift from EGIS Pharmaceutical Ltd.

Results

NK1R+ neurons labelled by TMR-substance P

To label NK1R+ neurons in lamina I and lamina III/IV in the dorsal horn, spinal cord slices were incubated with fluorescent TMR-substance P for 20 min and washed with Krebs solution for at least 20 min. NK1R+ neurons were identified under fluorescence microscopy by comparing their shapes and locations under IR-DIC and the CY3 filters as shown in Fig. 1*C* and *D*. Only the brightest cells were selected for recording. Usually 5–15 brightly labelled cells in lamina I and 3–10 brightly labelled cells in lamina III/IV could be identified on each side of the slice with 2–5 of them at a good depth for recording.

To test whether prelabelling of dorsal horn neurons with TMR-substance P significantly changes the synaptic currents under study, we recorded EPSCs before labelling lamina I neurons. After observing AMPA receptor-mediated monosynaptic input associated with dorsal root stimulation, TMR-substance P (40 nM) was added to the bath while continuing to record synaptic input. Four neurons tested in this way (4/10 neurons) became labelled with TMR-substance P (data not shown) and thus were identified as NK1R+. No systematic change in holding current was observed. Two of the four tested cells showed slight depression of AMPA EPSC amplitudes,

and one showed transient depression of RI that quickly recovered upon washout of TMR-substance P. Earlier studies by Bennett & Simmons (2001) demonstrated good binding of TMR-substance P to cells expressing NK1R, but poor ability to inhibit M-current in bullfrog sympathetic ganglion neurons. However, TMR-substance P was able to evoke Ca^{2+} transients in NK1R-expressing CHO cells in the same study (Bennett & Simmons, 2001). Nevertheless, under the conditions of our experiments, TMR-substance P appears to have no gross impact on the ratio of Ca^{2+}-permeable and -impermeable AMPA receptors of NK1R+ neurons.

The expression of TRPV1 receptors on primary afferents terminating on lamina I, lamina III/IV NK1R+ neurons and lamina I NK1R– neurons

The TRPV1 receptor is an important marker for nociceptors. It is activated by capsaicin and noxious heat and it can integrate temperature and pH changes (Caterina *et al.* 1997, 2000; Tominaga *et al.* 1998). To confirm our earlier observations that many lamina I and some lamina III/IV NK1R+ neurons receive primary afferent input from fibres containing functional TRPV1 receptors (Labrakakis & MacDermott, 2003), and to determine the impact of activated TRPV1 receptors on evoked glutamate release, capsaicin (1 μM), a TRPV1 receptor agonist, was superfused onto the spinal cord slices and its effect on evoked EPSCs observed. Figure 2*A* shows the time course over which capsaicin depressed the evoked EPSCs recorded from a lamina I NK1R+ neuron. In 6/6 lamina I NK1R+ cells tested, capsaicin significantly inhibited monosynaptic EPSC amplitude with an average depression of $68 \pm 9\%$ ($P < 0.01$; Fig. 2*B*). In 6/7 lamina I NK1R– cells tested, capsaicin depressed EPSC amplitude by $85 \pm 8\%$ ($P < 0.01$, $n = 6$). In contrast, capsaicin inhibited the amplitude of evoked EPSCs recorded in lamina III/IV neurons by an average of $18 \pm 5\%$ ($n = 6/8$). We conclude that, under our slice conditions, both NK1R+ and NK1R– neurons in lamina I receive heat-sensitive nociceptive inputs, while NK1R+ neurons in lamina III/IV receive the majority of their primary afferent input from heat-insensitive fibres.

EPSCs recorded from lamina I, and lamina III NK1R+ and lamina I NK1R– neurons

Synaptic currents recorded from superficial dorsal horn neurons following dorsal root stimulation were complex in time course and ionic composition. Figure 3*A* shows evoked synaptic currents recorded at different holding potentials from a lamina I NK1R+ neuron. These currents show evidence that at least two synaptic components are present with different reversal potentials. Superfusion with the $GABA_A$ receptor antagonist, SR 95531 (5–10 μM), and the glycine receptor antagonist, strychnine (1 μM), decreased outward current at positive holding potentials and simplified the synaptic current waveforms to one with a single reversal potential, presumably glutamate receptor-mediated EPSCs (Fig. 3*B*).

To further dissect the excitatory EPSCs, D-APV, an NMDA receptor antagonist was applied. It blocked the slowly decaying component revealing non-NMDA receptor-mediated EPSCs (Fig. 3*C*). The

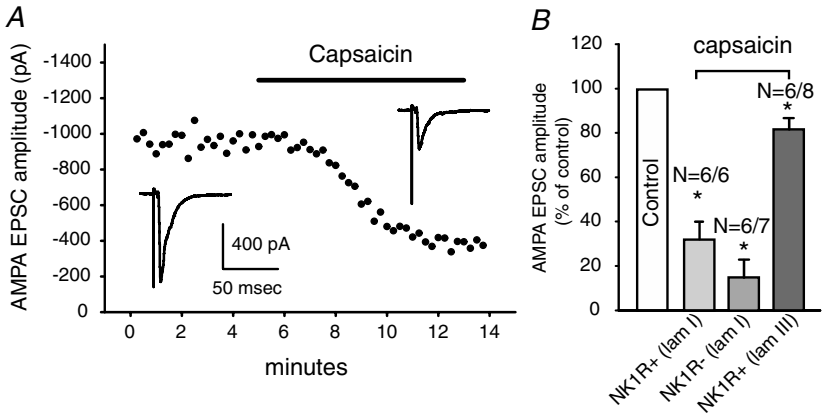

Figure 2. Lamina I neurons receive most of their inputs from TRPV1-expressing primary afferents while lamina III/IV neurons receive most inputs from TRPV1-lacking primary afferents
A, an example of the time course of the effect of capsaicin (1 μM) on the amplitude of evoked non-NMDA receptor-mediated EPSCs from an NK1R+ neuron in lamina I in the presence of SR 95531 (5 μM)/strychnine (1 μM)/D-APV (50 μM). The insets show evoked EPSCs before and during application of capsaicin. In this and all subsequent figures, traces are average of three events. *B*, averaged data showing the percentage of non-NMDA EPSC depression by capsaicin from lamina I NK1R+, NK1R– and lamina III/IV NK1R+ neurons. The numbers above each bar indicates the number of cells showing significant depression and the total number of cells tested. The error bars denote the standard error of the mean. Asterisks indicate significant difference compared to control.

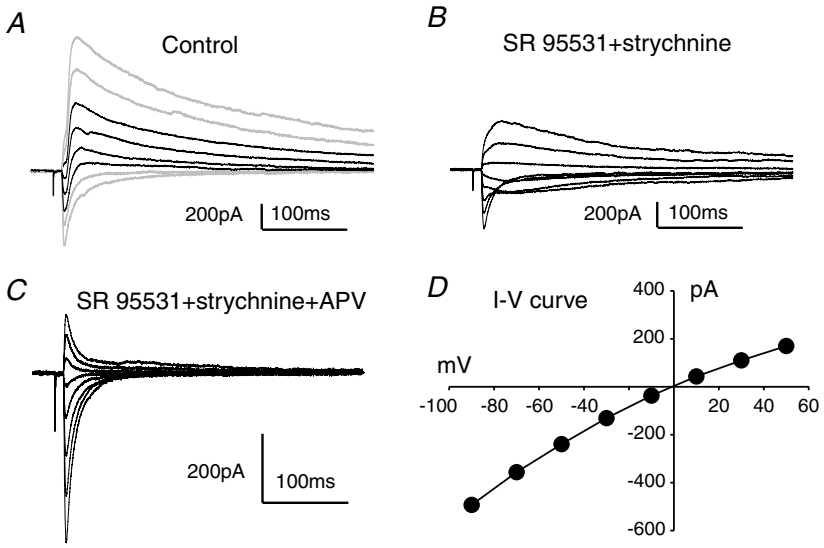

Figure 3. $GABA_A$/glycine, NMDA and non-NMDA receptor-mediated synaptic currents were evoked in NK1R+ neurons following dorsal root stimulation
A, synaptic currents evoked in an NK1R+ neuron in lamina I at different holding potentials (from −90 to +50 mV with 20 mV increments). The black traces show synaptic currents with two distinct reversal potentials. *B*, synaptic currents evoked from the same cell as in *A* but in SR 95531 (5 μM) + strychnine (1 μM). *C*, evoked EPSCs in the same cell as in *A* and *B* but further superfused with D-APV (50 μM). Non-NMDA receptor-mediated EPSCs were revealed. *D*, peak *I–V* relationship for the non-NMDA EPSCs obtained from *C*.

current–voltage relationship for these non-NMDA currents is shown in Fig. 3*D* with a reversal potential of 0 mV.

AMPA receptor antagonists GYKI 52466 (100 μM) and GYKI 53655 (50 μM) (Paternain *et al.* 1995) were found to largely block AMPA receptor-mediated EPSCs. GYKI 53655 reversibly diminished non-NMDA receptor-mediated EPSC amplitudes by 99% in the example shown from a lamina I NK1R+ neuron (Fig. 4*A*). On average, GYKI 53655 and GYKI 52466 diminished non-NMDA receptor-mediated EPSC amplitudes by $99 \pm 4\%$ ($n = 4$) and $94 \pm 3\%$ ($n = 3$), respectively, as shown in Fig. 4*B*. This suggests that AMPA receptors carry the majority of the current during non-NMDA receptor-mediated EPSCs. To further confirm that kainate receptors contribute little to these synaptic currents, SYM 2081 (3 μM), the rapidly desensitizing kainate receptor agonist (Zhou *et al.* 1997; Donevan *et al.* 1998; Li *et al.* 1999) was tested on the AMPA EPSCs. SYM 2081 had no significant effect on the non-NMDA receptor-mediated EPSCs recorded from lamina I NK1R+ neurons ($4 \pm 2\%$ inhibition, $n = 4$, $P > 0.05$, data not shown). Thus, these fast EPSCs recorded in the presence of D-APV can be referred to as AMPA EPSCs.

We also recorded AMPA EPSCs evoked by primary afferent activation of lamina I neurons not expressing NK1R, or NK1R– neurons, and compared their characteristics to the lamina I NK1R+ neurons. AMPA EPSCs from the lamina I NK1R– neurons isolated in this way tended to have smaller amplitudes than NK1R+ neurons (Table 1). These smaller amplitudes were paralleled by smaller cell sizes as indicated by significantly lower neuronal capacitance (Table 1). As with lamina I NK1R+ neurons, GYKI 53655 and GYKI 52466 depressed non-NMDA EPSCs by 98% ($n = 1$) and $92 \pm 5\%$ ($n = 3$), respectively (Fig. 4*B*), demonstrating that the majority of non-NMDA receptors at the primary afferent to NK1R– neuron synapses are also AMPA receptors.

For NK1R+ neurons in lamina III/IV, pharmacologically isolated AMPA EPSCs from 20 lamina III/IV NK1R+ neurons showed significantly faster rise times than those recorded from lamina I NK1R+

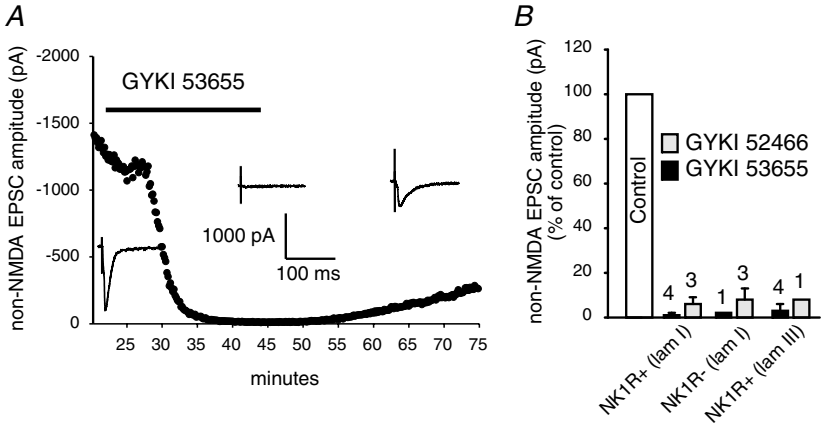

Figure 4. AMPA receptors are the primary non-NMDA receptors that mediate synaptic transmission between primary afferents and different subpopulations of dorsal horn neurons
A, time course of the effect of 50 μM GYKI 53655 on evoked non-NMDA receptor-mediated EPSCs recorded from a lamina I NK1R+ neuron. The insets show evoked EPSCs before, during and after application of GYKI 53655. *B*, the bar graph shows the average blocking effect of 50 μM GYKI 53655 or 100 μM GYKI 52466 on non-NMDA receptor-mediated EPSC amplitudes. The numbers above each bar indicate the numbers of cells tested. The error bars indicate the standard error of the mean.

Table 1. Synaptic and membrane properties of three subpopulations of dorsal horn neurons

	Rise time (ms)	Peak amplitude (pA)	Reversal potential (mV)	Capacitance (pF)	*n*	Rectification index (mean ± S.E.M., range)
Lamina I NK1R+	3.4 ± 0.4†	601 ± 98	0.2 ± 0.5	45.4 ± 3.7*	44–47	0.78 ± 0.04*, 0.44–1.68
Lamina I NK1R–	2.3 ± 0.3	300 ± 89	0.2 ± 0.5	25.5 ± 3.1	9	0.62 ± 0.06, 0.43–0.92
Lamina III/IV NK1R+	1.3 ± 0.1†	345 ± 60	0.2 ± 0.8	22.5 ± 2.8	20 (14) (6)	0.71 ± 0.04, 0.24–0.89 0.64 ± 0.05, 0.50–0.83

Rise time and peak amplitude values for each neuron were measured from a synaptic trace representing an average of three consecutive events recorded while holding membrane potential at −70 mV. Means of values obtained from the three populations of neurons are given ± standard error of the mean. *n* represents the number of neurons from each population used in this analysis. The two sets of RI values given for lamina III/IV neurons are for the two populations of neurons. *indicates that this value is significantly higher than that of the other two groups. The pair of † symbols in the rise time column indicates that these two numbers are significantly different.

neurons. The average amplitude of AMPA EPSCs for the lamina III/IV neurons tended to be smaller than that of lamina I NK1R+ neurons and similar to EPSC amplitudes of lamina I NK1R– neurons (Table 1). This again was paralleled by significantly smaller cell capacitance of lamina III/IV NK1R+ neurons, compared to lamina I NK1R+ neurons (Table 1). GYKI 53655 and GYKI 52466 depressed non-NMDA EPSCs by 97 ± 3% ($n = 4$) and 92% ($n = 1$), respectively (Fig. 4*B*), suggesting that the major non-NMDA receptor-mediated component at this synapse was mediated by AMPA receptors.

Some of the synaptic AMPA receptors are Ca^{2+} permeable

AMPA receptors can be Ca^{2+} permeable or impermeable, depending on their subunit composition (Hollmann *et al.* 1991). In studies using heterologous expression systems, Ca^{2+}-permeable AMPA receptors, composed of homomeric or heteromeric GluR1, GluR3 or GluR4 subunits, have RI values of 0.07–0.45. Ca^{2+}-impermeable AMPA receptors, which contain GluR2 subunits, have RIs of 1.5–3.2 (Verdoorn *et al.* 1991). To determine whether Ca^{2+}-permeable AMPA receptors are present at synapses between primary afferent fibres and subpopulations of dorsal horn neurons, the RI was calculated. Because inward rectification of Ca^{2+}-permeable AMPA receptors is due to intracellular voltage-dependent block of the channel by spermine (Kamboj *et al.* 1995; Koh *et al.* 1995), 100 μM spermine was always included in the patch pipette.

A range of RIs was observed within each of the three subpopulations of dorsal horn neurons studied. Figure 5 shows a comparison of the degree of rectification in two examples each from NK1R+ and NK1R– neurons in lamina I. The current–voltage relationship of synaptic currents from the first example shows moderate inward rectification (Fig. 5*A*; RI = 0.50), indicating that Ca^{2+}-permeable AMPA receptors contribute some of the synaptic current. Figure 5*B* shows synaptic currents recorded from another NK1R+ neuron in lamina I, but in this case the curve shows outward rectification (RI = 1.17), indicating few Ca^{2+}-permeable AMPA receptors are present. In 47 NK1R+ neurons tested in lamina I, the RIs ranged from 0.44 to 1.68 (Fig. 5*E*; Table 1).

AMPA EPSCs evoked with primary afferent input onto NK1R– neurons in lamina I had an overlapping range of RIs compared to the NK1R+ neurons (Fig. 5*E*). Figure 5*C* shows the current–voltage relationship from one lamina I NK1R– neuron with strong inward rectification (RI = 0.46), while Fig. 5*D* shows an example of a neuron with little rectification (RI = 0.91). The range of RIs from nine NK1R– neurons is 0.43–0.92, with an average value of 0.62 ± 0.06. This is significantly lower than the average RI for lamina I NK1R+ neurons (0.78 ± 0.04), indicating that overall, these lamina I NK1R– neurons express more synaptic Ca^{2+}-permeable AMPA receptors than the NK1R+ neurons.

Monosynaptic AMPA EPSCs were recorded from 20 lamina III/IV NK1R+ neurons, following stimulation of primary afferents. Of these 20 neurons, 14 were similar to synaptic currents already described from lamina I neurons, and had RI values ranging between 0.24 and 0.89 with an average value of 0.71 ± 0.04. An example of a current–voltage relationship for synaptic currents recorded from such a neuron is shown in Fig. 6*A*. The other 6 of the 20 neurons had AMPA EPSCs with two distinct reversal potentials, as shown in the example in Fig. 6*B*. Reversal potential for the first peak averaged around +1 mV, and the second averaged around +11 mV. For these neurons, RI was calculated using the first monosynaptic peak EPSC that reversed near 1 mV. RI values ranged from 0.5 to 0.83, with an average value of 0.64 ± 0.05. All 20 neurons had RIs less than 1.0 (Fig. 6*C*). This is consistent with earlier reports that Ca^{2+}-permeable AMPA receptors are expressed by some lamina III/IV neurons, although the populations of neurons were not identified in those earlier studies (Engelman *et al.* 1999).

To confirm that RI can predict the presence of Ca^{2+}-permeable AMPA receptors at synapses between primary afferent fibres and dorsal horn neurons, JSTX-3 (3 μM) or philanthotoxin-433 (40 μM), Ca^{2+}-permeable, non-NMDA receptor open channel blockers, were tested for their effect on the amplitude of AMPA EPSCs. Because these polyamines can only block the receptor-coupled channels that are open, 1 Hz stimulation for 60 s was delivered 2–3 times before and during drug application. For a neuron with strong inward rectification, the amplitude of AMPA EPSCs was not changed by the 1 Hz trains before polyamine application. However, the stimuli allowed significant depression of AMPA EPSC amplitudes during polyamine application (Fig. 7*A*). For cells with little inward rectification, polyamines were unable to depress AMPA EPSC amplitudes during 1 Hz trains (Fig. 7*B*). The relationship between the percentage depression of EPSC amplitude by polyamines, and the degree of inward rectification prior to blocker application is shown in Fig. 7*C*. Synaptic currents with low RIs were depressed by the blocker, while those with high RIs were resistant.

Discussion

We have investigated the synaptic currents recorded from three populations of pre-identified dorsal horn neurons and driven by single brief stimuli to dorsal roots in rat spinal cord slice preparations. Two of these groups of neurons, the NK1R+ neurons in lamina I and lamina III/IV of the dorsal horn, are known to be required for expression of some forms of hyperalgesia and allodynia (Nichols *et al.* 1999). Some of these neurons had been previously shown to express Ca^{2+}-permeable AMPA receptors, but it was unknown whether they were expressed at synapses and, if so, which ones. Therefore, we tested the hypothesis that afferent input onto NK1R+ neurons in both lamina I and lamina III/IV was mediated by Ca^{2+}-permeable AMPA receptors. Based on pharmacological and electrophysiological evidence,

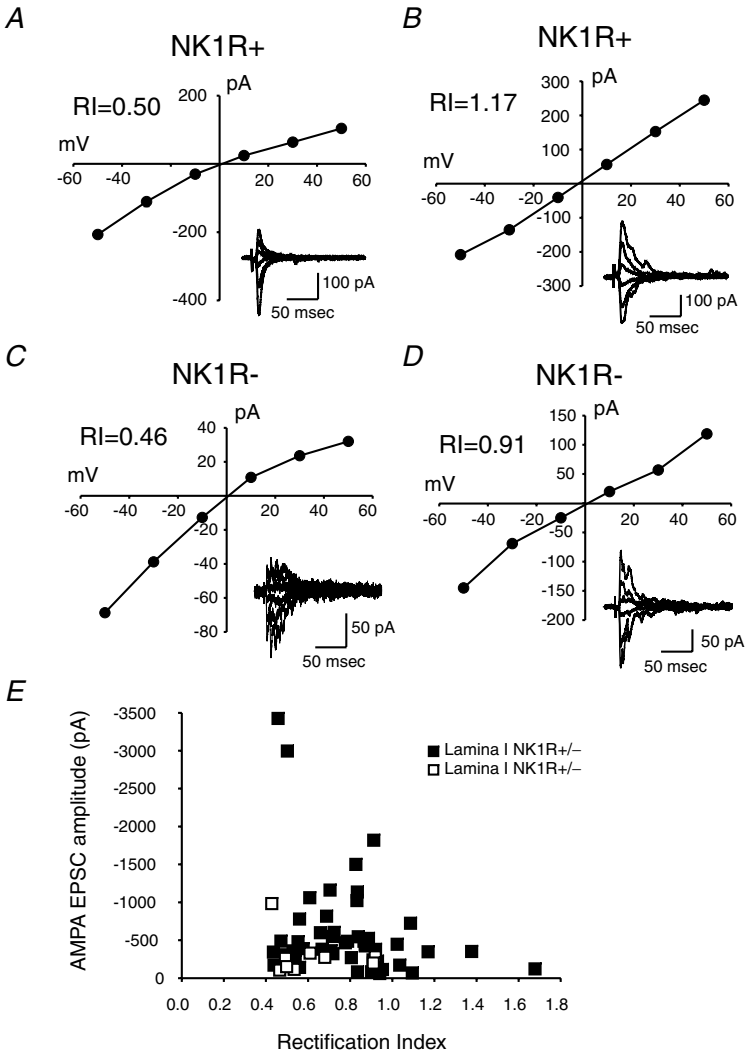

Figure 5. Different synapses between primary afferents and lamina I neurons show different degrees of rectification
RI, rectification index. *A*, an example of peak *I–V* for evoked AMPA EPSCs recorded from an NK1R+ neuron. Inset is the corresponding AMPA EPSC traces. *B*, an example of peak *I–V* from another NK1R+ neuron. *C*, an example of an *I–V* curve for evoked AMPA EPSCs recorded from an NK1R– neuron. *D*, an example of an *I–V* curve for evoked AMPA EPSCs recorded from another NK1R– neuron. *E*, distribution of AMPA EPSC amplitudes as a function of RI for lamina I NK1R+ and NK1R– neurons. The mean RI of EPSCs for NK1R+ neurons is higher than that for NK1R– neurons.

we conclude that the postsynaptic AMPA receptors at primary afferent synapses onto the NK1R+ neurons in lamina I and lamina III/IV, as well as the control NK1R– neurons in lamina I, include variable mixtures of both Ca^{2+}-permeable and Ca^{2+}-impermeable AMPA receptors.

Identification of presynaptic partners

Lamina I NK1R+ neurons receive monosynaptic input predominantly from Aδ and C fibres (Torsney & MacDermott, 2006), while lamina III/IV neurons receive both Aδ/C and Aβ fibre input (Naim *et al.* 1997, 1998; Torsney & MacDermott, 2006). We focused our studies on Aδ fibre-mediated monosynaptic primary afferent input to lamina I and Aβ fibre input to lamina III/IV NK1R+ neurons. Stimulation at 10 Hz of the dorsal roots was used to identify monosynaptic responses by their constant latency and lack of failure of the synaptic responses. Aβ afferent fibres can easily follow 10 Hz stimulation with an action potential for each stimulus, while 10% of Aδ fibres and 60% of C fibres fail to follow (Nakatsuka *et al.* 2000). It is therefore likely that some neurons receiving C fibre-mediated monosynaptic inputs were not included in this study. However, these criteria ensured that all of the synapses included in the analysis were monosynaptic connections between primary afferents and selected dorsal horn neurons, and most are likely to be monosynaptic inputs from primary afferent A fibres to lamina I and lamina III/IV neurons.

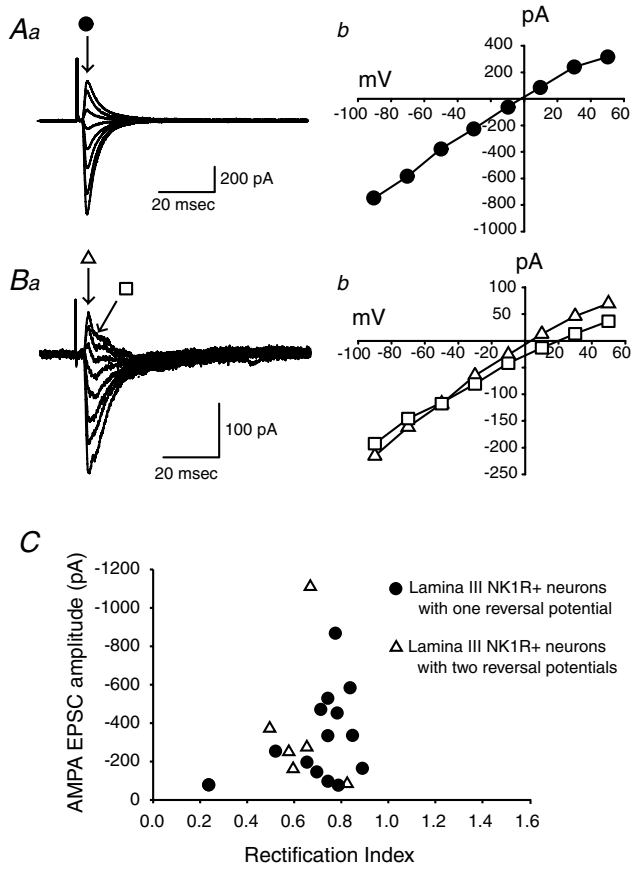

Figure 6. The synapses between primary afferents and NK1R+ neurons in lamina III/IV show two types of evoked EPSCs
Aa, an example of the first type of evoked AMPA EPSCs at different holding potentials. ● indicates the time point to measure the peaks of the AMPA EPSCs. *Ab*, peak current amplitudes are plotted as a function of membrane potential. *Ba*, an example of another type of AMPA EPSC. Evoked AMPA EPSCs showed two distinct reversal potentials. △ and □ indicate the time points to measure the first and second peak amplitudes of the AMPA EPSCs, respectively. *Bb*, peak *I–V* curves for the first and second peak amplitudes. *C*, distribution of AMPA EPSC amplitudes as a function of rectification index for two groups of lamina III/IV NK1R+ neurons.

TRPV1 channels are expressed on primary afferent fibres and terminals innervating lamina I NK1R+ neurons (Labrakakis & MacDermott, 2003), especially those projecting to lateral parabrachial nucleus (Hwang *et al.* 2003). In our studies, capsaicin depressed AMPA EPSC amplitudes by 68% and 85% of lamina I NK1R+ and NK1R– neurons, respectively. Because we are selecting primarily for A fibre input, this capsaicin-mediated depression is likely to be due to the presence of TRPV1 on intermediate-conducting, Aδ fibres. Even though TRPV1 is strongly expressed on C fibres (Guo *et al.* 1999), our results are consistent with observations showing that capsaicin depresses compound action potentials of intermediate-conducting fibres recorded from rat dorsal roots by 35%, as well as slow-conducting fibres by 85% (Labrakakis *et al.* 2003).

Capsaicin did not affect faster-conducting, presumably Aβ, fibres (Labrakakis *et al.* 2003). Because capsaicin only depressed AMPA EPSC amplitudes recorded from lamina III/IV NK1R+ neurons by an average of 18%, it is likely that the major primary afferent input of lamina III/IV NK1R+ neurons is TRPV1-negative fast-conducting Aβ fibres. However, the small depression of EPSC amplitude was significant in six of seven neurons tested, suggesting many of the lamina III/IV neurons in this study also received a small portion of their afferent input from higher-threshold fibres expressing TRPV1. Together, these data confirm that most of the fibres innervating lamina I NK1R+ and NK1R– neurons, as well as some of the fibres innervating lamina III/IV NK1R+ neurons, are sensitive to noxious heat, and they are likely to be in the Aδ class of afferents.

Identification of postsynaptic partners

All of our experiments were performed on pre-identified neurons in lamina I and lamina III/IV of the dorsal horn, based on evidence for strong expression, or clear lack of expression, of the NK1 receptor. The similarities

and differences among these groups are instructive. One difference is the cell size as suggested by capacitance values. The lamina I NK1R+ neurons, averaging 45 pF, were significantly larger than the lamina I NK1R– and lamina III/IV NK1R+ neurons. Earlier morphological studies show that NK1R+ neurons in lamina I fall into two groups, those expressing high levels and low levels of NK1R. Those lamina I neurons expressing high levels of NK1R are described as having large somas with several principal dendrites (Cheunsuang & Morris, 2000). Because the lamina I NK1R+ neurons we chose had the brightest cell bodies and high capacitance, it may be that our prelabelling technique reveals the neurons expressing high levels of NK1R.

The bulk of the lamina III/IV NK1R+ neurons, in addition to the lamina I NK1R– neurons, show significantly smaller cell capacitance, around 22 and 25 pF, respectively. The AMPA EPSCs of these smaller groups have significantly lower RI values than those of the lamina I NK1R+ neurons, indicating higher levels of Ca^{2+}-permeable AMPA receptor expression at these primary afferent synapses. Earlier reports indicate that Ca^{2+}-permeable AMPA receptors are moderately expressed by some NK1R+ neurons and strongly expressed by many GABAergic neurons in dorsal horn neuron culture (Albuquerque *et al.* 1999; Engelman *et al.* 1999). NK1R– neurons in lamina I could be either excitatory or inhibitory interneurons. Disinhibition of C fibre activation of deep dorsal horn neurons by a low dose of JSTX (Stanfa *et al.* 2000) is consistent with the idea that Ca^{2+}-permeable AMPA receptors could mediate synaptic excitatory drive onto inhibitory neurons in the dorsal horn. It may be therefore that at least some of the NK1R– neurons showing stronger inward rectification of AMPA EPSCs and smaller capacitance in our study are GABAergic neurons expressing Ca^{2+}-permeable AMPA receptors.

Ca^{2+}-permeable and -impermeable AMPA receptors at dorsal horn synapses

Although several studies have functionally demonstrated expression of Ca^{2+}-permeable AMPA receptors by many neurons in the superficial dorsal horn (Engelman *et al.*

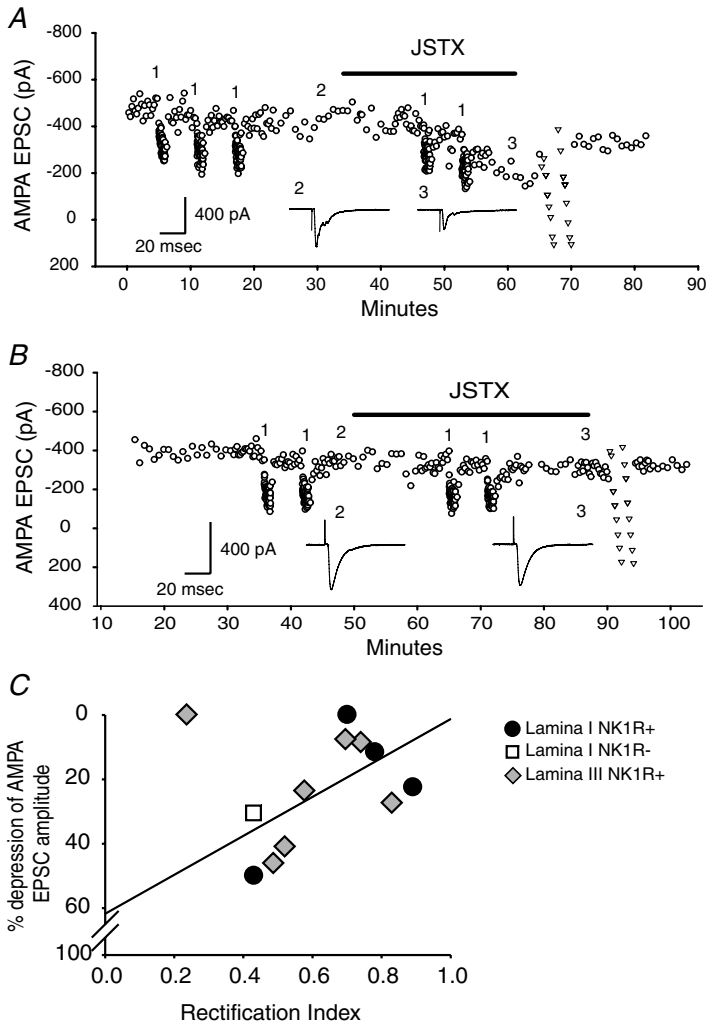

Figure 7. Ca^{2+}-permeable AMPA receptor antagonists depressed AMPA EPSC amplitudes showing strong inward rectification
A, application of JSTX-3 (3 μM) depressed AMPA EPSCs recorded from an NK1R+ neuron (RI = 0.49) in lamina III/IV by about 47%. Low-frequency stimuli (1 Hz for 1 min) were delivered during JSTX-3 application to open Ca^{2+}-permeable AMPA receptor channel. The number 1 indicates low-frequency stimuli; 2 denotes AMPA EPSCs before drug application; 3 denotes AMPA EPSCs recorded at the end of drug application. ▽ indicates *I–V* test at the end of the drug application. The insets show evoked EPSCs before and at the end of JSTX application. *B*, JSTX-3 did not have an effect on AMPA EPSCs recorded from another NK1R+ neuron showing higher RI (RI = 0.74) in lamina III/IV. *C*, a significant correlation ($P < 0.05$) between RI and percentage of AMPA EPSC depression by Ca^{2+}-permeable AMPA receptor antagonists. The regression line is plotted without the outlier.

1999; Hartmann *et al.* 2004), GluR2 is expressed at essentially all glutamatergic synapses there (Nagy *et al.* 2004). Because the presence of GluR2 within an AMPA receptor tetramer blocks Ca^{2+} permeability, this raises an apparent conflict with the cobalt loading studies showing widespread expression of Ca^{2+}-permeable AMPA receptors in the dorsal horn. One resolution to the paradox could be that Ca^{2+}-permeable AMPA receptors are expressed extrasynaptically, while Ca^{2+}-impermeable AMPA receptors are expressed at synapses. However, our results suggest the more likely explanation that Ca^{2+}-permeable AMPA receptors are expressed together with Ca^{2+}-impermeable receptors at primary afferent synapses. The wide range of RI values found for synaptic AMPA receptors within each population of neurons studied shows that the synaptic AMPA receptors that include GluR2 subunits and are Ca^{2+} impermeable coexist with receptors that do not include GluR2 and thus are Ca^{2+} permeable.

Compared with other dendritically localized Ca^{2+}-permeable channels such as NMDA receptors and voltage-gated Ca^{2+} channels, Ca^{2+}-permeable AMPA receptors have increased current flow when the membrane potential is more negative. It is therefore possible that with low-frequency input from primary afferent fibres, the predominant route of Ca^{2+} entry will be through Ca^{2+}-permeable AMPA receptors. When repetitive action potential activity drives glutamate release from presynaptic terminals, NMDA receptors and voltage-gated Ca^{2+} channels will contribute more strongly to intracellular Ca^{2+} accumulation. Thus Ca^{2+} signalling in dendrites through these different channels is dependent on activity. Furthermore, the contribution of Ca^{2+}-permeable AMPA receptors to Ca^{2+} entry and their functional roles in regulation of synaptic plasticity largely depend on their relative locations at synapses, and the morphology of dendrites (Goldberg & Yuste, 2005).

Evidence suggesting that Ca^{2+}-permeable AMPA receptors could contribute to enhanced excitability associated with synaptic activation was reported by Gu *et al.* (1996). Furthermore, enhanced excitatory drive requiring Ca^{2+}-permeable AMPA receptors is consistent with the reported role of Ca^{2+}-permeable AMPA receptors in expression of some forms of behavioural hyperalgesia and allodynia (Sorkin *et al.* 1999; Jones & Sorkin, 2004). For example, when Ca^{2+}-permeable AMPA receptors are strongly expressed between low-threshold fibres and some lamina III/IV NK1R+ neurons, they may contribute to the development of allodynia, which is defined as a pain sensation caused by non-noxious stimulation.

In each of the three neuronal subpopulations studied, there is a range of relative levels of expression of Ca^{2+}-permeable and -impermeable synaptic AMPA receptors, indicated by the range of RIs found. Recent experiments have shown that at some synapses, the relative proportion of these two forms of AMPA receptor can be rapidly altered by activity (Liu & Cull-Candy, 2000, 2005). For example, high-frequency stimulation of parallel fibre input to cerebellar stellate neurons causes a rapid decrease in synaptic Ca^{2+}-permeable AMPA receptors at mixed receptor synapses (Liu & Cull-Candy, 2000). Conversely, enhanced relative expression of Ca^{2+}-permeable AMPA receptors occurs over hours when activity is blocked in hippocampal cultured neurons (Thiagarajan *et al.* 2005). These observations suggest that the relative proportions of Ca^{2+}-permeable and -impermeable receptors at synapses in the superficial dorsal horn may not be a static property of particular synaptic partners. Rather, they may be more reflective of prior levels of activity. These possibilities remain to be tested at any glutamatergic synapses in the spinal cord dorsal horn.

Physiological impact of synaptic Ca^{2+}-permeable AMPA receptors expressed by NK1R+ neurons

The role of NK1R+ neurons in pain signalling is not fully understood. Behavioural studies show that NK1R+ neurons, not NK1 receptors, are important for allodynia and hyperalgesia development (Mantyh *et al.* 1997; De Felipe *et al.* 1998). Although morphological evidence shows there are two groups of lamina I NK1R+ neurons (Cheunsuang & Morris, 2000), there are no significant differences among lamina I NK1R+ neurons in their innervation by substance P-containing fibres or TRPV1-expressing fibres nor in their c-Fos response to noxious peripheral stimuli (Todd *et al.* 2002; Hwang *et al.* 2003), suggesting that NK1R+ neurons in lamina I may share a common role in the development of hypersensitivity. In contrast, lamina III/IV NK1R+ neurons show two subpopulations for their c-Fos expression, morphology and axonal projections (Doyle & Hunt, 1999). Differential expression of Ca^{2+}-permeable AMPA receptors by different subpopulations of superficial dorsal horn neurons in different sensory pathways may be important to selectively modulate their synaptic strength or other synaptic properties, which subsequently influences the generation of hyperalgesia or allodynia.

References

Albuquerque C, Lee CJ, Jackson AC & MacDermott AB (1999). Subpopulations of GABAergic and non-GABAergic rat dorsal horn neurons express Ca^{2+}-permeable AMPA receptors. *Eur J Neurosci* **11**, 2758–2766.

Bennett VJ & Simmons MA (2001). Analysis of fluorescently labeled substance P analogs: binding, imaging and receptor activation. *BMC Chem Biol* **1**, 1.

Caterina MJ, Leffler A, Malmberg AB, Martin WJ, Trafton J, Petersen-Zeitz KR, Koltzenburg M, Basbaum AI & Julius D (2000). Impaired nociception and pain sensation in mice lacking the capsaicin receptor. *Science* **288**, 306–313.

Caterina MJ, Schumacher MA, Tominaga M, Rosen TA, Levine JD & Julius D (1997). The capsaicin receptor: a heat-activated ion channel in the pain pathway. *Nature* **389**, 816–824.

Cheunsuang O & Morris R (2000). Spinal lamina I neurons that express neurokinin 1 receptors: morphological analysis. *Neuroscience* **97**, 335–345.

De Felipe C, Herrero JF, O'Brien JA, Palmer JA, Doyle CA, Smith AJ, Laird JM, Belmonte C, Cervero F & Hunt SP (1998). Altered nociception, analgesia and aggression in mice lacking the receptor for substance P. *Nature* **392**, 394–397.

Donevan SD, Beg A, Gunther JM & Twyman RE (1998). The methylglutamate, SYM 2081, is a potent and highly selective agonist at kainate receptors. *J Pharmacol Exp Ther* **285**, 539–545.

Doyle CA & Hunt SP (1999). Substance P receptor (neurokinin-1)-expressing neurons in lamina I of the spinal cord encode for the intensity of noxious stimulation: a c-Fos study in rat. *Neuroscience* **89**, 17–28.

Engelman HS, Allen TB & MacDermott AB (1999). The distribution of neurons expressing calcium-permeable AMPA receptors in the superficial laminae of the spinal cord dorsal horn. *J Neurosci* **19**, 2081–2089.

Goldberg JH & Yuste R (2005). Space matters: local and global dendritic Ca^{2+} compartmentalization in cortical interneurons. *Trends Neurosci* **28**, 158–167.

Gu JG, Albuquerque C, Lee CJ & MacDermott AB (1996). Synaptic strengthening through activation of Ca^{2+}-permeable AMPA receptors. *Nature* **381**, 793–796.

Guo A, Vulchanova L, Wang J, Li X & Elde R (1999). Immunocytochemical localization of the vanilloid receptor 1 (VR1): relationship to neuropeptides, the P2X3 purinoceptor and IB4 binding sites. *Eur J Neurosci* **11**, 946–958.

Hartmann B, Ahmadi S, Heppenstall PA, Lewin GR, Schott C, Borchardt T, Seeburg PH, Zeilhofer HU, Sprengel R & Kuner R (2004). The AMPA receptor subunits GluR-A and GluR-B reciprocally modulate spinal synaptic plasticity and inflammatory pain. *Neuron* **44**, 637–650.

Hollmann M, Hartley M & Heinemann S (1991). Ca^{2+} permeability of KA–AMPA-gated glutamate receptor channels depends on subunit composition. *Science* **252**, 851–853.

Hwang SJ, Burette A & Valtschanoff JG (2003). VR1-positive primary afferents contact NK1-positive spinoparabrachial neurons. *J Comp Neurol* **460**, 255–265.

Jones TL & Sorkin LS (2004). Calcium-permeable alpha-amino-3-hydroxy-5-methyl-4-isoxazolepropionic acid/kainate receptors mediate development, but not maintenance, of secondary allodynia evoked by first-degree burn in the rat. *J Pharmacol Exp Ther* **310**, 223–229.

Kamboj SK, Swanson GT & Cull-Candy SG (1995). Intracellular spermine confers rectification on rat calcium-permeable AMPA and kainate receptors. *J Physiol* **486**, 297–303.

Koh DS, Burnashev N & Jonas P (1995). Block of native Ca^{2+}-permeable AMPA receptors in rat brain by intracellular polyamines generates double rectification. *J Physiol* **486**, 305–312.

Labrakakis C & MacDermott AB (2003). Neurokinin receptor 1-expressing spinal cord neurons in lamina I and III/IV of postnatal rats receive inputs from capsaicin sensitive fibers. *Neurosci Lett* **352**, 121–124.

Labrakakis C, Tong CK, Weissman T, Torsney C & MacDermott AB (2003). Localization and function of ATP and $GABA_A$ receptors expressed by nociceptors and other postnatal sensory neurons in rat. *J Physiol* **549**, 131–142.

Li P, Wilding TJ, Kim SJ, Calejesan AA, Huettner JE & Zhuo M (1999). Kainate-receptor-mediated sensory synaptic transmission in mammalian spinal cord. *Nature* **397**, 161–164.

Liu SQ & Cull-Candy SG (2000). Synaptic activity at calcium-permeable AMPA receptors induces a switch in receptor subtype. *Nature* **405**, 454–458.

Liu SJ & Cull-Candy SG (2005). Subunit interaction with PICK and GRIP controls Ca^{2+} permeability of AMPARs at cerebellar synapses. *Nat Neurosci* **8**, 768–775.

Mantyh PW, Rogers SD, Honore P, Allen BJ, Ghilardi JR, Li J, Daughters RS, Lappi DA, Wiley RG & Simone DA (1997). Inhibition of hyperalgesia by ablation of lamina I spinal neurons expressing the substance P receptor. *Science* **278**, 275–279.

Nagy GG, Al-Ayyan M, Andrew D, Fukaya M, Watanabe M & Todd AJ (2004). Widespread expression of the AMPA receptor GluR2 subunit at glutamatergic synapses in the rat spinal cord and phosphorylation of GluR1 in response to noxious stimulation revealed with an antigen-unmasking method. *J Neurosci* **24**, 5766–5777.

Naim MM, Shehab SA & Todd AJ (1998). Cells in laminae III and IV of the rat spinal cord which possess the neurokinin-1 receptor receive monosynaptic input from myelinated primary afferents. *Eur J Neurosci* **10**, 3012–3019.

Naim M, Spike RC, Watt C, Shehab SA & Todd AJ (1997). Cells in laminae III and IV of the rat spinal cord that possess the neurokinin-1 receptor and have dorsally directed dendrites receive a major synaptic input from tachykinin-containing primary afferents. *J Neurosci* **17**, 5536–5548.

Nakatsuka T, Ataka T, Kumamoto E, Tamaki T & Yoshimura M (2000). Alteration in synaptic inputs through C-afferent fibers to substantia gelatinosa neurons of the rat spinal dorsal horn during postnatal development. *Neuroscience* **99**, 549–556.

Nichols ML, Allen BJ, Rogers SD, Ghilardi JR, Honore P, Luger NM, Finke MP, Li J, Lappi DA, Simone DA & Mantyh PW (1999). Transmission of chronic nociception by spinal neurons expressing the substance P receptor. *Science* **286**, 1558–1561.

Paternain AV, Morales M & Lerma J (1995). Selective antagonism of AMPA receptors unmasks kainate receptor-mediated responses in hippocampal neurons. *Neuron* **14**, 185–189.

Pogatzki EM, Niemeier JS, Sorkin LS & Brennan TJ (2003). Spinal glutamate receptor antagonists differentiate primary and secondary mechanical hyperalgesia caused by incision. *Pain* **105**, 97–107.

Sorkin LS, Yaksh TL & Doom CM (1999). Mechanical allodynia in rats is blocked by a Ca^{2+}-permeable AMPA receptor antagonist. *Neuroreport* **10**, 3523–3526.

Stanfa LC, Hampton DW & Dickenson AH (2000). Role of Ca^{2+}-permeable non-NMDA glutamate receptors in spinal nociceptive transmission. *Neuroreport* **11**, 3199–3202.

Thiagarajan TC, Lindskog M & Tsien RW (2005). Adaptation to synaptic inactivity in hippocampal neurons. *Neuron* **47**, 725–737.

Todd AJ, Puskar Z, Spike RC, Hughes C, Watt C & Forrest L (2002). Projection neurons in lamina I of rat spinal cord with the neurokinin 1 receptor are selectively innervated by substance P-containing afferents and respond to noxious stimulation. *J Neurosci* **22**, 4103–4113.

Tominaga M, Caterina MJ, Malmberg AB, Rosen TA, Gilbert H, Skinner K, Raumann BE, Basbaum AI & Julius D (1998). The cloned capsaicin receptor integrates multiple pain-producing stimuli. *Neuron* **21**, 531–543.

Torsney C & MacDermott AB (2006). Disinhibition opens the gate to pathological pain signalling in superfiical NK1 receptor expressing neurons in rat spinal cord. *J Neurosci* **26**, 1833–1843.

Verdoorn TA, Burnashev N, Monyer H, Seeburg PH & Sakmann B (1991). Structural determinants of ion flow through recombinant glutamate receptor channels. *Science* **252**, 1715–1718.

Zhou LM, Gu ZQ, Costa AM, Yamada KA, Mansson PE, Giordano T, Skolnick P & Jones KA (1997). (2S,4R)-4-methylglutamic acid (SYM 2081): a selective, high-affinity ligand for kainate receptors. *J Pharmacol Exp Ther* **280**, 422–427.

Acknowledgements

This work was supported by a National Institutes of Health grant NS 029797 and grant C018608 from the New York State Department of Health Spinal Cord Injury Research Board. We thank Dr Carole Torsney and Claire Daniele for their comments on the manuscript, and Asya Haney for technical assistance.